Am J Cancer Res 2022;12(8):4074-4081
www.ajcr.us /ISSN:2156-6976/ajcr0143937

Brief Communication

Pan-cancer profiles of the cuproptosis gene set

Hengrui Liu

Biocomma Limited, Shenzhen, China

Received May 5, 2022; Accepted July 16, 2022; Epub August 15, 2022; Published August 30, 2022

Abstract: A recent study has revealed a novel cell death pathway, called "cuproptosis", a programmed cell death based on copper. A total of 12 genes were involved in the cuproptosis pathway, including 7 pro-cuproptosis genes (FDX1, LIAS, LIPT1, DLD, DLAT, PDHA1, and PDHB) genes, 3 anti-cuproptosis genes (MTF1, GLS, and CDKN2A), and 2 key copper transporters ATP7B and SLC31A1. The insight into these cuproptosis genes in cancer is necessary to understand cuproptosis-related tumorigenesis and to develop the cuproptosis pathway as a potential therapeutic target for clinical cancer treatment. By mining multi-omic profiling data, we performed a comprehensive and systematic characterization of the cuproptosis of these 12 genes across more than 9000 samples of 33 types of cancer. This letter not only revealed diverse mechanisms of the gene expression regulations of the cuproptosis gene set in cancer but also analyzed the potential associations between cuproptosis and other common cancer pathways, providing an overall picture of cuproptosis in cancer for future reference. This study comprehensively clarified the genomic pan-cancer profiles of the cuproptosis gene set regarding the SNV, CNV, methylation, mRNA expression, pathway cross-talk, and miRNA regulations across 33 solid tumors. Our findings revealed that genomic alterations and miRNA-mRNA network-mediated ectopic expression of cuproptosis genes were involved in the activation of other cancer-related pathways and also identified KIRC as a potential cancer type that might be affected by cuproptosis. We think, as the rase of the cuproptosis cancer research, these in-time profiles will provide a genetic overview and useful information for future studies on the cuproptosis in cancers.

Keywords: Cuproptosis, cancers, genes, clinical

Introduction

A recent paper [1] has revealed a novel cell death pathway, called "cuproptosis", a programmed cell death based on copper, that is different from known cell death pathways such as apoptosis, necrosis, oncosis, pyroptosis, autophagy, and ferroptosis. Copper served as a co-factor for a number of key enzymes across almost all organisms [2], but the homeostatic level of intracellular copper is strictly regulated, and the accumulation of intracellular free copper can result in the death of cells [3, 4]. The intracellular concentration of copper has been found to affect many types of cancers, such as breast cancer [5], head and neck cancer [6], and endometrial cancer [7], however, only until the recent publication did the pathway of cuproptosis sorted out with a set of cuproptosis genes identified. A total of 10 genes were involved in the cuproptosis pathway, including 7 pro-cuproptosis genes (FDX1, LIAS, LIPT1, DLD, DLAT, PDHA1, and PDHB) genes and 3 anti-cuproptosis genes (MTF1, GLS, and CDKN2A) [1]. In addition, two key copper transporters are key cuproptosis affecting genes, including copper exporter ATP7B [8] and copper importer SLC31A1 [9]. The insight into these cuproptosis genes in cancer is necessary to understand cuproptosis-related tumorigenesis and to develop the cuproptosis pathway as a potential therapeutic target for clinical cancer treatment. By mining multi-omic profiling data, we performed a comprehensive and systematic characterization of the cuproptosis of these 12 genes across more than 9000 samples of 33 types of cancer. This letter not only revealed diverse mechanisms of the gene expression regulations of the cuproptosis gene set in cancer but also analyzed the potential associations between cuproptosis and other common cancer pathways, providing an overall picture of cuproptosis in cancer for future reference. The detailed methods of the analyses were provided in the Supplementary Materials. We think, as the rase of the cuproptosis cancer research,

these in-time profiles will provide a genetic overview and useful information for future studies on the cuproptosis in cancers.

Results and discussions

Pan-cancer single nucleotide variation profiles of cuproptosis gene set

The single nucleotide variation (SNV) analysis revealed that CDKN2A was the most frequently mutated cuproptosis gene across cancer types, especially in HNSC and PAAD, where the mutation rate was over 20%. ATP7B was the second most frequently mutated cuproptosis gene in cancer. Generally, UCEC had a relatively higher mutation rate in all cuproptosis genes than other cancer types (**Figure 1A**). The SNV landscape showed that most of the SNVs were missense-mutation, followed by a small proportion of other mutation types such as nonsense-mutation, except for the most frequently mutated gene, CDKN2A, which had a relatively high proportion of nonsense-mutation (**Figure 1B**). The profile of the survival association of cuproptosis gene SNVs revealed that the cancer types that were most likely to associate with cuproptosis genes SNV were BRCA and COAD. However, only a few genes were significant, and, for most of the other cancer types, no significance was found (**Figure 1D**). Based on the SNV analysis, although CDKN2A had a high SNV frequency, we suggested that the SNVs in cuproptosis genes might not be critical for cancers.

Pan-cancer copy number variation profiles of cuproptosis gene set

The copy number variation (CNV) profile showed that the CNV of the cuproptosis gene set across different cancer types had a variety of patterns. The pan-cancer pie chart and CNV plots of the cuproptosis gene set showed that the major CNV types were heterozygous CNV, with only very few cases of homozygous CNV (**Figure 1D-F**). The profile of the survival association of cuproptosis gene CNVs revealed that the cancer types that were most likely to associate with cuproptosis genes CNV were UCEC, KIRP, and ACC. However, for the other cancer types, there were only a few significances in part of the cuproptosis gene set (**Figure 1G**). The correlation profile of CNV and expression demonstrated that, for most cancer types, CNV was positively correlated with expressions of most of the cuproptosis genes (**Figure 1H**). Based on the CNV analysis, we suggested that the heterozygous CNV might potentially associate with cancers, especially in UCEC, KIRP, and ACC where cuproptosis genes CNV correlated with the survival of patients.

Pan-cancer methylation profiles of cuproptosis gene set

The profile of the methylation differences between tumor and normal tissues revealed that a few cancer types had a difference in methylation of some cuproptosis genes between tumor and normal tissues but there were no cancer-noncancer difference patterns shared across different cancer types (**Figure 1I**). The correlation profile of methylation and mRNA expression revealed that a few cancer types had significant correlations between methylation and mRNA expression in some cuproptosis genes and most of these correlations were negative correlations (**Figure 1J**). The survival correlation analysis of methylation showed that the methylation levels were not correlated with the survival of cancer in most cancer types (**Figure 1K**). Based on the CNV analysis, we suggested that hypermethylation was one of the potential mechanisms of down-regulation of some cuproptosis genes, but, overall, the methylation level of cuproptosis gene set was not closely associated with cancers.

Pan-cancer gene expression profiles of cuproptosis gene set

We analyzed the expression difference of cuproptosis genes between cancer and noncancer tissues from TCGA. Results showed that KIRC had the most significantly different genes. DLD, PDHA1, GLS, DLAT, SLC31A1, PDHB, and FDX1 were down-regulated in KIRC, while CDKN2A and ATP7B were up-regulated in KIRC. CDKN2A was the gene that was significantly different between normal and cancer in most of the cancer types across all cuproptosis genes. Yet, for most cancer types, there were only a few significant differences in the expression of these genes between cancer and their non-cancer tissues (**Figure 2A**). We also analyzed the expression of these genes among cancer subtypes, results revealed that BRCA, KIRC, STAD, and LUAD were the top four cancer types that showed significance (**Figure**

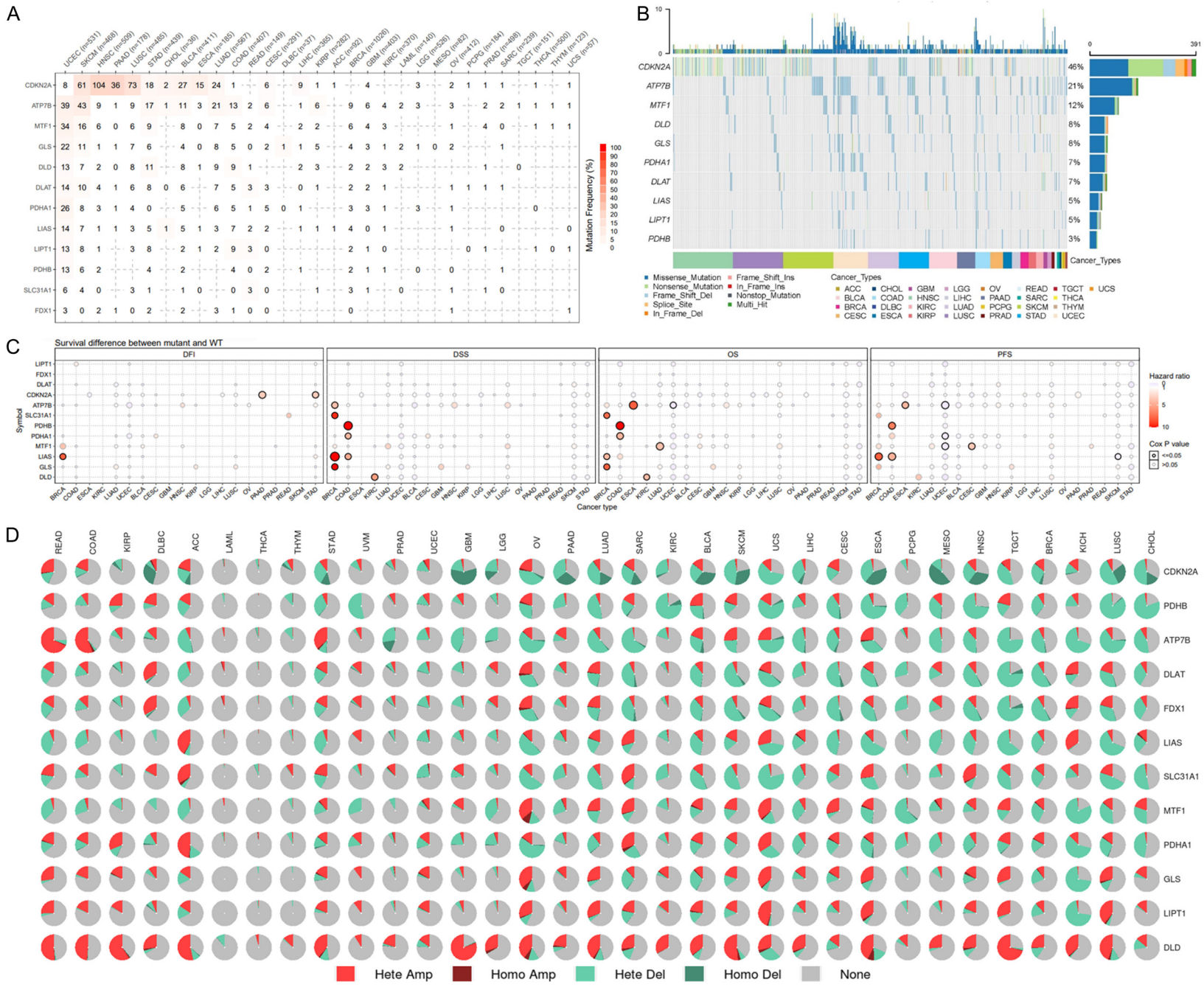
A
B
C
D
Survival difference between mutant and WT
DFI
DSS
OS
PFS
Hazard ratio
Cox P value
Cancer type
Mutation Frequency (%)
Cancer_Types
Missense_Mutation
Nonsense_Mutation
Frame_Shift_Del
Splice_Site
In_Frame_Del
Frame_Shift_Ins
In_Frame_Ins
Nonstop_Mutation
Multi_Hit
Hete Amp
Homo Amp
Hete Del
Homo Del
None

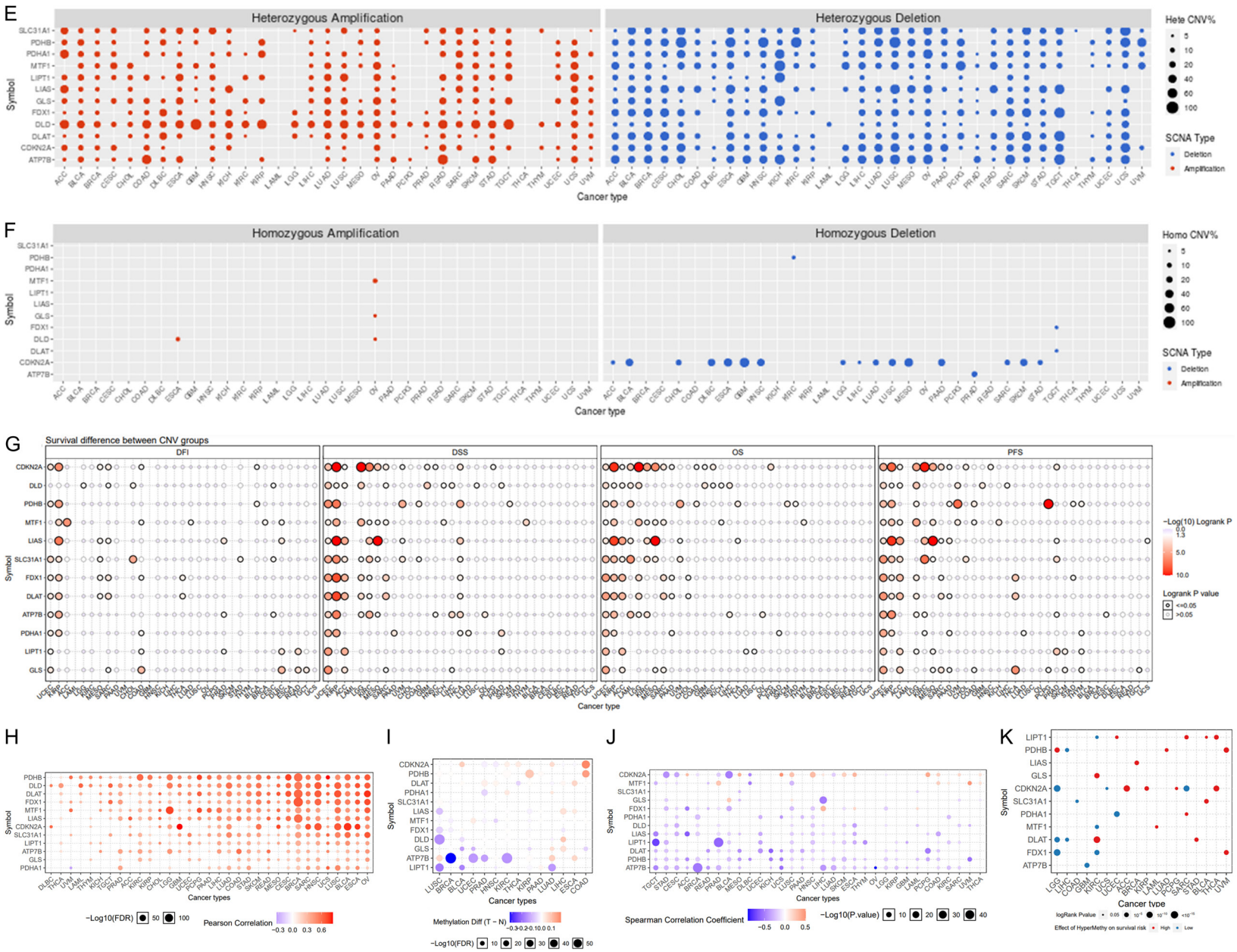
E
Heterozygous Amplification
Heterozygous Deletion
Hete CNV%
SCNA Type
Deletion
Amplification
Symbol
Cancer type
F
Homozygous Amplification
Homozygous Deletion
Homo CNV%
G
Survival difference between CNV groups
DFI
DSS
OS
PFS
−Log(10) Logrank P
Logrank P value
H
I
J
K
Cancer types
Spearman Correlation Coefficient
Methylation Diff (T − N)
Effect of HyperMethy on survival risk

Figure 1. Pan-cancer genetic profiles of cuproptosis gene set. A. Heatmap of the mutation frequency. Numbers represent the number of samples that have the corresponding mutated gene for a given cancer. "0" indicates that there was no mutation in the gene coding region, blank indicates there was no mutation in any region of the gene, and color represents the mutation frequency. B. The SNV landscaped plot of cuproptosis genes in cancers. C. Survival difference between mutant and wild-type cuproptosis genes. Copy number variation (CNV) and methylation analysis of cuproptosis genes in cancers. D. CNV distribution pie chart across cancers. Hete Amp = heterozygous amplification; Hete Del = heterozygous deletion; Homo Amp = homozygous amplification; Homo Del = homozygous deletion; None = no CNV. E, F. Heterozygous and homozygous CNV profile showing the percentage of amplification and deletion of heterozygous and homozygous CNVs for each gene in each cancer. Only genes with >5% CNV in a given cancer are shown as a point in the figure. G. Survival difference between CNV groups. H. The correlation of CNV and mRNA expression. I. Methylation differences between tumor and normal tissues. J. The correlation of methylation and mRNA expression. K. Survival difference between samples with high and low methylation of cuproptosis genes (only significant cancer types were plotted).

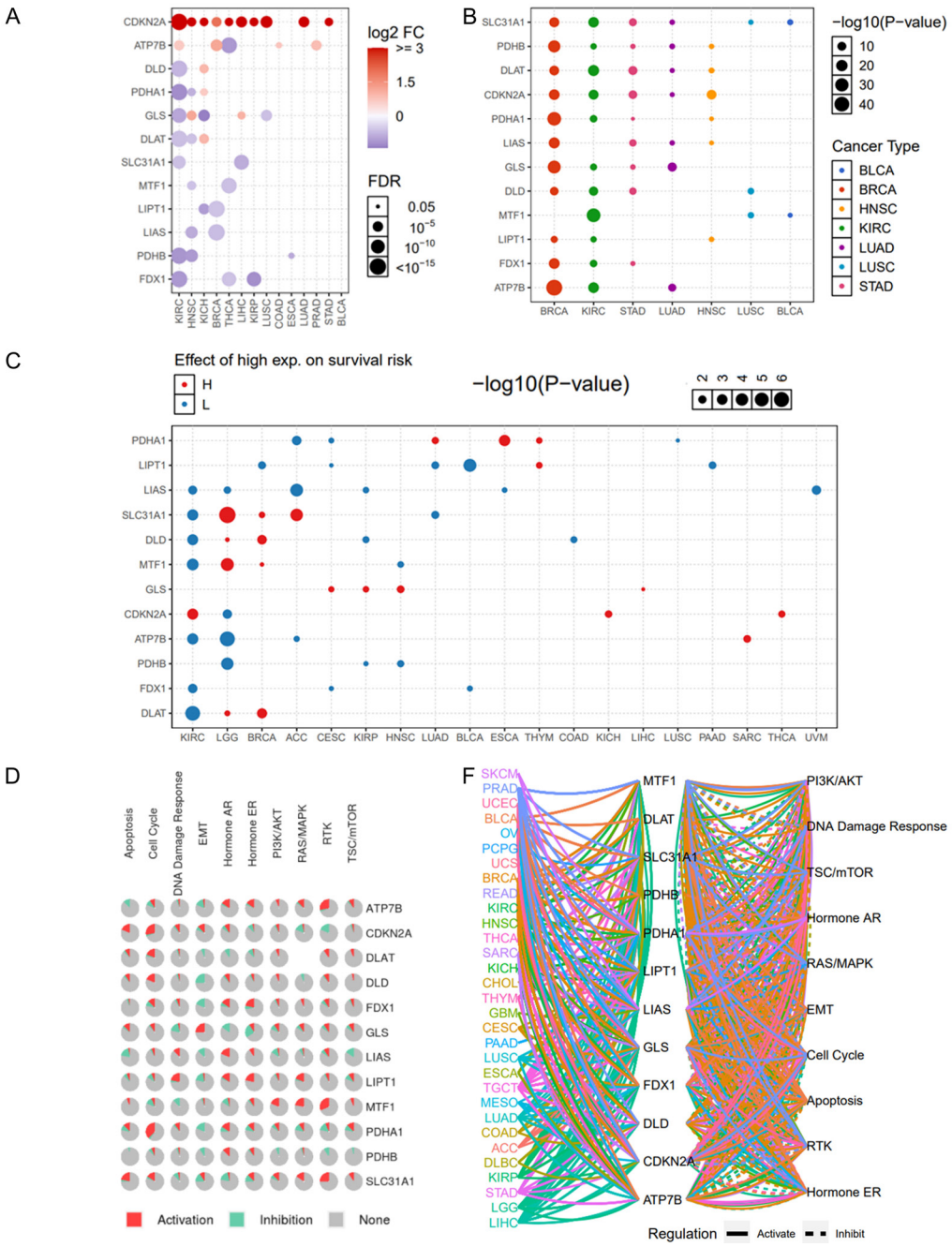

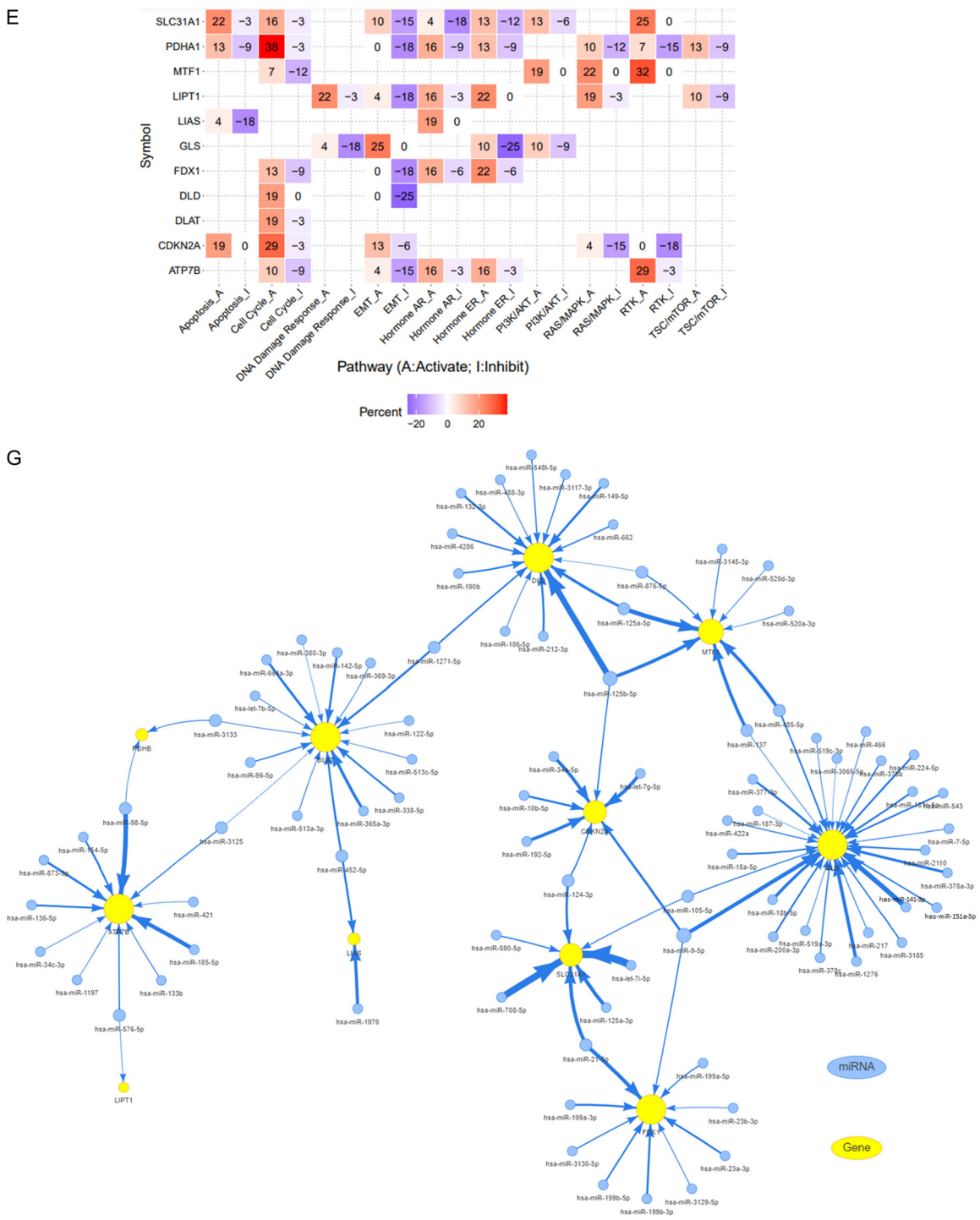

Figure 2. Pan-cancer expression and cross-talk profiles of cuproptosis gene set. A. Expression difference between cancer and non-cancer tissues from TCGA. B. Expression differences between subtypes of cancers. C. Survival difference between high and low expression groups. D. Pie chart of the percentage of the effect of cuproptosis gene cross-talk with other cancer pathway activity. E. Heat map of the percentage of the effect of cuproptosis genes on other cancer pathway activity. F. Pathway regulation network of cuproptosis genes. A line represents a connection between genes and different pathways, where a solid line represents activation, and a dashed line represents inhibition. The color of the line represents different cancer types. G. The microRNA (miRNA) network of cuproptosis genes. A miRNA and one regulator connection node represent miRNA regulation of a gene. Node size is positively correlated with the node's degree, and edge width is defined by the absolute value of the correlation coefficient.

2B). Survival analysis showed that KIRP was the cancer type whose survival was the most associated with cuproptosis genes. The high expressions of five pro-cuproptosis genes (LIAS, SLC31A1, DLD, FDX1, and DLAT) and two anti-cuproptosis genes (MTF1 and ATP7B) were associated with a low survival risk in KIRP, while the expression of anti-cuproptosis gene CDKN2A was associated with a high survival risk in KIRP. In addition, LGG was another cancer type whose survival might associate with cuproptosis, yet, for the other cancer types, there were only a few significances in survival associations (**Figure 2C**). These expression analyses identified KIRC as a potential cancer type that might be affected by cuproptosis.

Pan-cancer pathway cross-talk profiles of cuproptosis gene set

To explore the potential cross-talk of cuproptosis and other cancer-related pathways, we analyzed the reverse-phase protein array (RPPA) data from the TCPA database to calculate scores for 7876 cancer samples and provided pan-cancer pathway cross-talk profiles of the cuproptosis gene set. As shown in the pie chart, the cuproptosis genes were also potentially involved in the activations of other cancer pathways, but most of these involvements were not remarkable except for a few genes in some pathways, such as PDHA1 in the cell cycle, MTF1 in RTK, ATP7B in RTK, and CDKN2A in the cell cycle (**Figure 2D**). Detailed percentage numbers of the activation and inactivation of these pathways were presented in **Figure 2D**. A pan-cancer pathway regulation network of cuproptosis genes was also constructed based on these results (**Figure 2F**). These pathway cross-talk profiles provided information on the potential connections between cuproptosis and other cancer-related pathways.

Pan-cancer pathway cross-talk profiles of cuproptosis gene set

This study also analyzed the miRNA expression data from TCGA and constructed a miRNA-regulation network of cuproptosis genes. Eleven of the twelve genes of the cuproptosis gene set were found in the databases with regulating miRNA. As shown in **Figure 2G**, multiple miRNAs might be involved in the regulation of the expression of the cuproptosis genes, including several co-regulators for some of the cuproptosis genes. ATP7B was regulated by 11 miRNA, where the top regulating miRNA were has-miR-185-5p and has-miR-98-5p. The has-miR-98-5p was also regulating PDHB and the has-miR-576-5p was regulating both ATP7B and LIPT1. DLAT was regulated by 15 miRNA, where the top regulating miRNA were has-miR-365a-3p, has-miR-664a-3p, and has-miR-1271-5p. has-miR-3133 was regulating both DLAT and PDHB and the has-miR-452-5p was regulating both DLAT and LIAS. The LIAS was only regulated by has-miR-452-5p and has-miR-1976. DLD was regulated by 14 miRNA, whose top regulated miRNA was has-miR-125b-5p, a miRNA that also regulated MTF1 and CDKN2A. Similar to has-miR-125b-5p, has-miR-876-5p and has-miR-125a-5p regulated both DLD and MTF1. CDKN2A was also regulated by multiple other miRNAs. FDX1 was regulated by 10 miRNA and the top regulating one was has-miR-21-5p, which was also regulating SLC31A1. SLC31A1 was regulated by 7 miRNA, especially by has-miR-708-5p and has-let-7i-5p. GAS has the most regulating miRNA. It was regulated by 27 miRNA, where the top correlated miRNAs were has-miR-9-5p, a miRNA also regulated CDKN2 and FDX1, and has-miR-141-3p (**Figure 2G**). The network provided an overview of the potential cuproptosis-regulating miRNAs for future reference.

Conclusions

This study comprehensively clarified the genomic pan-cancer profiles of the cuproptosis gene set regarding the SNV, CNV, methylation, mRNA expression, pathway cross-talk, and miRNA regulations across 33 solid tumors. Our findings revealed that genomic alterations and miRNA-mRNA network-mediated ectopic expression of cuproptosis genes were involved in the activation of other cancer-related pathways and also identified KIRC as a potential cancer type that might be affected by cuproptosis. The pan-cancer analysis of cuproptosis genes may provide additional insight into novel clinical therapy targeting cuproptosis.

Acknowledgements

This study received funding from Biocomma Limited. The author thanks the support of Gaoming Chen, Weifen Chen, Zongxiong Liu, and Yaqi Yang.

Disclosure of conflict of interest

None.

Address correspondence to: Hengrui Liu, Biocomma Limited, Shenzhen, China. E-mail: hengrui.liu@biocomma.cn

References

[1] Tsvetkov P, Coy S, Petrova B, Dreishpoon M, Verma A, Abdusamad M, Rossen J, Joesch-Cohen L, Humeidi R, Spangler RD, Eaton JK, Frenkel E, Kocak M, Corsello SM, Lutsenko S, Kanarek N, Santagata S and Golub TR. Copper induces cell death by targeting lipoylated TCA cycle proteins. Science 2022; 375: 1254-1261.

[2] Kim BE, Nevitt T and Thiele DJ. Mechanisms for copper acquisition, distribution and regulation. Nat Chem Biol 2008; 4: 176-185.

[3] Ge EJ, Bush AI, Casini A, Cobine PA, Cross JR, DeNicola GM, Dou QP, Franz KJ, Gohil VM, Gupta S, Kaler SG, Lutsenko S, Mittal V, Petris MJ, Polishchuk R, Ralle M, Schilsky ML, Tonks NK, Vahdat LT, Van Aelst L, Xi D, Yuan P, Brady DC and Chang CJ. Connecting copper and cancer: from transition metal signalling to metalloplasia. Nat Rev Cancer 2022; 22: 102-113.

[4] Lutsenko S. Human copper homeostasis: a network of interconnected pathways. Curr Opin Chem Biol 2010; 14: 211-217.

[5] Jouybari L, Kiani F, Islami F, Sanagoo A, Sayehmiri F, Hosnedlova B, Doşa MD, Kizek R, Chirumbolo S and Bjørklund G. Copper concentrations in breast cancer: a systematic review and meta-analysis. Curr Med Chem 2020; 27: 6373-6383.

[6] Ressnerova A, Raudenska M, Holubova M, Svobodova M, Polanska H, Babula P, Masarik M and Gumulec J. Zinc and copper homeostasis in head and neck cancer: review and meta-analysis. Curr Med Chem 2016; 23: 1304-1330.

[7] Atakul T, Altinkaya SO, Abas BI and Yenisey C. Serum copper and zinc levels in patients with endometrial cancer. Biol Trace Elem Res 2020; 195: 46-54.

[8] Lukanović D, Herzog M, Kobal B and Černe K. The contribution of copper efflux transporters ATP7A and ATP7B to chemoresistance and personalized medicine in ovarian cancer. Biomed Pharmacother 2020; 129: 110401.

[9] Yu Z, Zhou R, Zhao Y, Pan Y, Liang H, Zhang JS, Tai S, Jin L and Teng CB. Blockage of SLC31A1-dependent copper absorption increases pancreatic cancer cell autophagy to resist cell death. Cell Prolif 2019; 52: e12568.

Supplementary Materials

Methods

Data acquisitions

The expression, methylation, single-nucleotide variant (SNV), and copy number variant (CNV) data with clinical information were downloaded from The Cancer Genome Atlas (TCGA) [1] and the UniProt. The reverse-phase protein array (RPPA) data were downloaded from the cancer proteome atlas (TCPA) [2, 3]. The miRNA regulation data of melatonergic regulators were collected from databases including experimentally verified (scientific papers, TarBase [4], miRTarBase [5], and mir2disease [6]) data, and targetscan and miRanda predicted data. The immune therapy survival data were accessed from the Tumor Immune Dysfunction and Exclusion (TIDE) [7, 8].

Gene alterations and expression analysis

All the expression and methylation analyses and plotting were implemented by R foundation for statistical computing (2020) version 4.0.3 and ggplot2 (v3.3.2) or accessed from the website of the data source. SNV plots were generated by the maftools [9]. CNV data were processed with GISTICS2.0 [10]. Data were analyzed using the t-test or ANOVA t-test. To compare the data, the integrated level of the expression of the cuproptosis gene set was calculated using the gene set variation analysis (GSVA) with the R package GSVA [11].

Survival analysis

The mRNA expression, methylation, and clinical survival data were analyzed. Tumor samples were divided into high and low groups according to the median gene RSEM value. The R package survival was used to fit the survival time and survival status for the two groups. A Cox Proportional-Hazards model was used to calculate survival risk (Hazard ratio, HR) for every gene. A log-rank test of Kaplan-Meier survival was performed for each gene.

Pathway activity analysis

Reverse-phase protein array (RPPA) data from the TCPA database were used to calculate scores for 7876 samples. Ten cancer-related pathways included tuberous sclerosis 1 protein (TSC)/mechanistic target of rapamycin (mTOR), receptor tyrosine kinase (RTK), phosphatidylinositol-4,5-bisphosphate-3-kinase (PI3K)/protein kinase B (AKT), RAS/mitogen-activated protein kinase (MAPK), hormone estrogen receptor (ER), hormone androgen receptor (AR), epithelial-mesenchyme transition (EMT), the DNA Damage Response, cell cycle, apoptosis pathways. The pathway score is the sum of the relative protein level of all positive regulatory components minus that of negative regulatory components in a particular pathway. The pathway activity score (PAS) was estimated as in previous studies [12, 13]; gene expression was divided into two groups (High and Low) by the median expression and the difference in PAS between groups was analyzed using Student's t-test where the *P*-value was adjusted by the FDR. The FDR $\leq$0.05 was considered significant. When PAS (Gene A group High) >PAS (Gene A group Low), gene A was considered to have an activating effect on this pathway; otherwise, it had an inhibitory effect on the pathway.

MicroRNA (miRNA) regulation network analysis

Only miRNA-gene pairs that have recorded data were used to calculate the expression correlation. The miRNA expression and gene expression were merged via the TCGA barcode. The association between paired mRNA and miRNA expression was tested based on a Pearson product-moment correlation coefficient and the t-distribution. The *P*-value was adjusted by the FDR and only significant connections were plotted. Correlations were calculated for all paired samples. Meanwhile, in consideration of the pres-

ence of positive regulators, including transcription factors, a miRNA-gene pair with a negative correlation will be considered as a potential negatively regulated pair. The network was constructed using the visNetwork R package.

Statistical analysis

All statistical analyses were performed using the R software v4.0.3. Correlation analysis was performed using the Spearman correlation test. A Cox proportional hazards model was used to calculate survival risk and hazard ratio (HR). The prognostic significance of every variable was estimated using Kaplan-Meier survival curves and compared using log-rank tests. Group comparisons were analyzed using T. test or ANOVA t-test. If not otherwise stated, the rank-sum test detected two sets of data, and a *P*-value <0.05 was considered statistically significant.

References

[1] Weinstein JN, Collisson EA, Mills GB, Shaw KR, Ozenberger BA, Ellrott K, Shmulevich I, Sander C and Stuart JM. The cancer genome atlas pan-cancer analysis project. Nat Genet 2013; 45: 1113-1120.

[2] Li J, Akbani R, Zhao W, Lu Y, Weinstein JN, Mills GB and Liang H. Explore, visualize, and analyze functional cancer proteomic data using the cancer proteome atlas. Cancer Res 2017; 77: e51-e54.

[3] Li J, Lu Y, Akbani R, Ju Z, Roebuck PL, Liu W, Yang JY, Broom BM, Verhaak RG, Kane DW, Wakefield C, Weinstein JN, Mills GB and Liang H. TCPA: a resource for cancer functional proteomics data. Nat Methods 2013; 10: 1046-1047.

[4] Karagkouni D, Paraskevopoulou MD, Chatzopoulos S, Vlachos IS, Tastsoglou S, Kanellos I, Papadimitriou D, Kavakiotis I, Maniou S, Skoufos G, Vergoulis T, Dalamagas T and Hatzigeorgiou AG. DIANA-TarBase v8: a decade-long collection of experimentally supported miRNA-gene interactions. Nucleic Acids Res 2018; 46: D239-D245.

[5] Huang HY, Lin YC, Li J, Huang KY, Shrestha S, Hong HC, Tang Y, Chen YG, Jin CN, Yu Y, Xu JT, Li YM, Cai XX, Zhou ZY, Chen XH, Pei YY, Hu L, Su JJ, Cui SD, Wang F, Xie YY, Ding SY, Luo MF, Chou CH, Chang NW, Chen KW, Cheng YH, Wan XH, Hsu WL, Lee TY, Wei FX and Huang HD. miRTarBase 2020: updates to the experimentally validated microRNA-target interaction database. Nucleic Acids Res 2020; 48: D148-D154.

[6] Jiang Q, Wang Y, Hao Y, Juan L, Teng M, Zhang X, Li M, Wang G and Liu Y. miR2Disease: a manually curated database for microRNA deregulation in human disease. Nucleic Acids Res 2009; 37: D98-D104.

[7] Fu J, Li K, Zhang W, Wan C, Zhang J, Jiang P and Liu XS. Large-scale public data reuse to model immunotherapy response and resistance. Genome Med 2020; 12: 21.

[8] Jiang P, Gu S, Pan D, Fu J, Sahu A, Hu X, Li Z, Traugh N, Bu X, Li B, Liu J, Freeman GJ, Brown MA, Wucherpfennig KW and Liu XS. Signatures of T cell dysfunction and exclusion predict cancer immunotherapy response. Nat Med 2018; 24: 1550-1558.

[9] Mayakonda A, Lin DC, Assenov Y, Plass C and Koeffler HP. Maftools: efficient and comprehensive analysis of somatic variants in cancer. Genome Res 2018; 28: 1747-1756.

[10] Mermel CH, Schumacher SE, Hill B, Meyerson ML, Beroukhim R and Getz G. GISTIC2.0 facilitates sensitive and confident localization of the targets of focal somatic copy-number alteration in human cancers. Genome Biology 2011; 12: R41.

[11] Hänzelmann S, Castelo R and Guinney J. GSVA: gene set variation analysis for microarray and RNA-seq data. BMC Bioinformatics 2013; 14: 7.

[12] Akbani R, Ng PK, Werner HM, Shahmoradgoli M, Zhang F, Ju Z, Liu W, Yang JY, Yoshihara K, Li J, Ling S, Seviour EG, Ram PT, Minna JD, Diao L, Tong P, Heymach JV, Hill SM, Dondelinger F, Städler N, Byers LA, Meric-Bernstam F, Weinstein JN, Broom BM, Verhaak RG, Liang H, Mukherjee S, Lu Y and Mills GB. A pan-cancer proteomic perspective on The Cancer Genome Atlas. Nat Commun 2014; 5: 3887.

[13] Ye Y, Xiang Y, Ozguc FM, Kim Y, Liu CJ, Park PK, Hu Q, Diao L, Lou Y, Lin C, Guo AY, Zhou B, Wang L, Chen Z, Takahashi JS, Mills GB, Yoo SH and Han L. The Genomic Landscape and Pharmacogenomic Interactions of Clock Genes in Cancer Chronotherapy. Cell Syst 2018; 6: 314-328, e312.